Article

Layered Inorganic/Enzyme Nanohybrids with Selectivity and Structural Stability upon Interacting with Biomolecules

Guo-Jing Chen, Ming-Cheng Yen, Jen-Ming Wang, Jiang-Jen Lin, and Hsin-Cheng Chiu

Bioconjugate Chem., **2008**, 19 (1), 138-144 • DOI: 10.1021/bc700224q • Publication Date (Web): 11 December 2007

Layered Inorganic/Enzyme Nanohybrids with Selectivity and Structural Stability upon Interacting with Biomolecules

Guo-Jing Chen, Ming-Cheng Yen, Jen-Ming Wang, Jiang-Jen Lin,† and Hsin-Cheng Chiu*

Department of Chemical Engineering, National Chung Hsing University, Taichung 402, Taiwan. Received June 20, 2007; Revised Manuscript Received November 1, 2007

Effective intercalation of protein molecules within the galleries of montmorillonites can be achieved via simple space enlarging and exchange processes while retaining the native conformation of the guest protein and the multilayered structure of the bioinert host plates. The capacity of accommodating protein molecules in the galleries can be markedly larger than that governed by the Langmuir-type adsorption of protein molecules on the external surfaces of particles. The basal spacing in the multilayered structure of clay is abruptly enlarged when the extent of protein intercalation increases to a critical point. Beyond this critical point, the nanohybrids show well-preserved catalytic activity in hydrolyzing small substrates while establishing a barrier to interactions with large biomacromolecules. Furthermore, the structural stability of the inorganic/organic nanohybrids is enhanced such that neither exchange of biomolecules nor exfoliation of layered clay particles occurs when exposed to other proteins. The results indicate that, through the benign accommodation of protein species between the inorganic platelets, this nanoscaled manipulation of protein functions can be highly useful in developing new inorganic/enzyme nanohybrids for protein therapeutics and tissue engineering.

INTRODUCTION

Inorganic/organic nanohybrids formed via accommodating bioactive macromolecules inside the galleries of inorganic materials with layered structure have found a variety of potential applications in biomedical and biochemical fields. For example, inorganic layered double hydroxide (LDH)/DNA hybrids can facilitate the endocytic uptake of DNA fragments and their intracellular release from the hybrids by complete dissolution of LDH in the acidic environment of endosomes (*1, 2*). Biologically active proteins such as enzymes incorporated in synthetic layered α-zirconium phosphate, while retaining their conformation and activity, have been found capable of acting as nanoscale biocatalytic systems (*3–9*). Mutual interactions between guest biomolecules and inorganic host plates occur mainly by electrostatic attraction (*10, 11*). Small DNA fragments and antisense oligonucleotides can be readily embedded within the galleries of cationic LDH layered structures by either direct anionic exchange or coprecipitation in the in situ formation of LDH layers (*1, 2*). The hybrids prepared from the latter approach can accommodate double-stranded DNAs over a wide range of molecular sizes (*2*). Similarly, owing to the three-dimensional size, large globular proteins can be successfully embedded within inorganic layered hosts only by self-assembly with synthetic exfoliated plates in aqueous phase into hybrids of double- or triple-layered structure (*3–8*). Hybrids with elevated stacking in the layered structure that act as highly efficient bioreactors have not been attainable due to the instability problem encountered. On the other hand, montmorillonite (MMT), one of the most abundant smectite clays, consists of aluminosilicate plates with dimensions of ca. $100 \times 100 \times 1$ nm^3 in each plate piling in a primary stack of ca. 8−10 layers through intensive charge attraction (*12*). Therefore, it is easily realized that, by taking the advantage of the high aspect ratio surface area of each layer within a multilayered structure, MMT may serve as a benign host to provide spacious sites for protein accommodation. Unfortunately, the basal spacing in multilayers of MMT homoionic, for example, to Na^+ (Na^+-MMT) is 1.2 nm. With the thickness of each layer equal to 1 nm, the interlayer free space is 0.2 nm. Interactions of the multilayered particles with such narrow galleries and most large globular proteins are inevitably restricted to their external bulk surfaces. The incorporation of guest biomolecules in the clay galleries is therefore severely limited in variety and adsorption/intercalation capacity.

In this study, inorganic/enzyme hybrids were obtained by a simple exchange process of the protein molecules with an originally intercalated linear synthetic polymer within the spatially enlarged galleries of MMT. Taking advantages of its globular structure and catalytic activity in hydrolyzing both low molecular weight and macromolecular substrates, α-chymotrypsin (CHT) was employed as a model protein intercalant. In addition to detailed characterization of morphology and structure of the hybrids, the selectivity and stability of the hybrids regarding interactions with biomolecules of varying sizes was studied.

EXPERIMENTAL SECTION

Materials. CHT (EC 3.4.21.2, type II, from bovine pancreas), bovine serum albumin (BSA), catalase (from bovine liver), *N*-benzoyl-L-tyrosine *p*-nitroanilide (Bz-Tyr-NAp), and *N*-succinyl-L-phenylalanine *p*-nitroanilide (Su-Phe-NAp) were purchased from Sigma. α,ω-Diaminopoly(oxypropylene) (POP, Mw 2000 g/mol) was obtained from Aldrich. Na^+-MMT with a cationic exchange capacity (CEC) of 1.15 mequiv/g was obtained from Kunimine. Deionized water used in the protein intercalation, and buffer preparation was prepared from Milli-Q Synthesis (Millipore). All other chemicals were reagent grade and used as received.

Inorganic/Enzyme Hybrid Preparation. Preparation of the inorganic/enzyme hybrids was carried out first by spatial enlargement of the galleries of MMT via cationic exchange of

* To whom correspondence should be addressed. E-mail: hcchiu@dragon.nchu.edu.tw (H.-C. Chiu).

† Current address of J. J. Lin: Institute of Polymer Science and Engineering, National Taiwan University, Taipei, Taiwan 106.

10.1021/bc700224q CCC: $40.75
Published on Web 12/11/2007

POP with sodium counterions within the galleries of MMT, followed by exchange of POP with the CHT molecules. The POP intercalation was performed as described previously (*13*). In brief, to a Na^+-MMT slurry in deionized water was added the aqueous solution of POP/HCl (1:1 in mole ratio) to a stoichimetric ratio of POP/CEC at 1.0 with stirring at 80 °C for 24 h. The inorganic/organic weight ratio of the MMT/POP hybrids was determined to be 31/69 by thermal gravimetric analysis. The mechanism of the POP intercalation and structure of MMT/POP hybrids have been studied in detail previously (*13–15*). The intercalation/adsorption of CHT on MMT/POP and Na^+-MMT particles, respectively, was performed by the addition of a prescribed amount of CHT in the aqueous clay suspension solutions (4.7 mg of Na^+-MMT in 15 mL phosphate buffer (pH 7.0, I 0.01 M) or 15.0 mg/15 mL of MMT/POP, equivalent to 4.7 mg of clay in 15 mL of the aqueous solution) at 4 °C for 12 h with stirring. The inorganic/enzyme composite particles were subjected repeatedly to centrifugation (10 000 g at 4 °C for 30 min) and resuspension with phosphate buffer and deionized water until protein in the supernatant was no longer detected. The products were then collected by lyophilization and stored at −20 °C for further characterization of their structure and enzymatic activity. The extent of the protein intercalation/adsorption was determined by measuring the protein concentration in the combined supernatants via the Bradford protein assay (Bio-Rad protein assay reagent) at 596 nm. The intercalation/adsorption isotherms were established by plotting the amount of CHT intercalated/adsorbed per gram of clay (μmol/g clay) versus the equilibrium CHT concentration (μM) in aqueous solution, i.e., the protein concentration in the supernatant after the equilibrium adsorption. The released amount of POP from the MMT/POP composite particles in protein intercalation was estimated by gel permeation chromatography (GPC) measurements (Superose 12, FPLC, GE-Pharmacia, the eluent: Tris buffer, 0.4 mL/min, RI detection) of the POP concentration in the supernatant of the first centrifugation.

Structural and Morphologic Characterization. The X-ray powder diffraction measurements of the MMT/CHT hybrids were performed using a powder diffractometer (Mac Science MXP-18) with a Cu target at 30 kV and 20 mA. The basal spacing was determined from their reflections (00l, $l = 1, 2, 3$, etc.) using the Bragg's law ($l\lambda = 2d \sin\theta$). For the atomic force microscopic (AFM) image analyses, the sample was suspended in deionized water (10^{-6} mg/mL) and spin-coated on the surfaces of glass substrate. The measurement was performed with scanning probe microscopy (SPM, dynamic force mode, Seiko, SPI 3800N) using rectangular Si cantilevers with 129 kHz resonant frequency and 12 N/m spring constant (Seiko, SI-DF20).

Enzymatic Activity Characterization. The hybrids were first tested for activity in catalytic hydrolysis of two small substrates, namely, Bz-Tyr-NAp and Su-Phe-NAp. The substrate stock solutions were prepared in DMSO at a concentration of 5.0×10^{-3} M. The reaction was performed in Tris buffer (0.08 M Tris + 0.01 M $CaCl_2$, pH 8.0) at 37 °C with a DMSO content less than 5.0% (v/v) of the incubation mixtures. The enzyme concentration in the reaction solution was 2.0×10^{-7} M, unless stated otherwise. The release of *p*-nitroaniline was monitored at 410 nm, and its molar absorptivity of 8800 M^{-1} cm^{-1} at this wavelength was employed to calculate its concentration over time (*16*). The kinetic parameters were obtained according to the Michaelis–Menten kinetic model, and each set of kinetic measurements was performed in duplicate with eight different substrate concentrations.

For the activity of the hybrids toward biomacromolecules, reactions were carried out with the concentrations of substrates (BSA and catalase, respectively) of 5 mg/mL and of CHT 2×10^{-5} M in Tris buffer at 37 °C. The MMT/CHT hybrids with a degree of CHT intercalation of 176 μmol/g clay were used. The extents of cleavage at different time intervals were evaluated in terms of the reduction (%) of the molecular peak of the substrates with respect to that at $t = 0$ in the GPC measurements under UV detection at 280 nm (*16*).

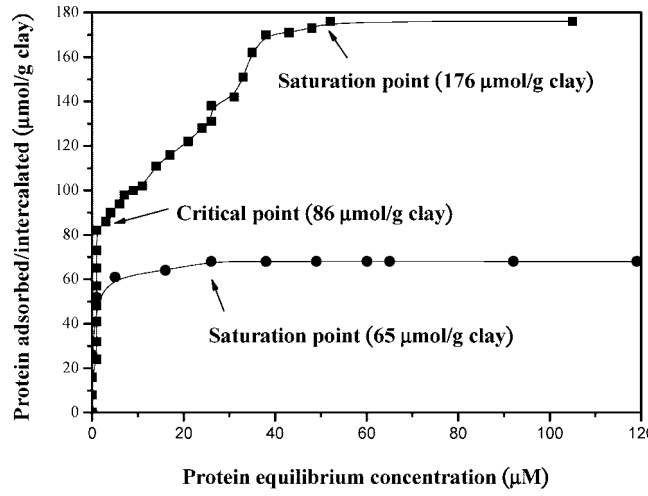

Figure 1. Adsorption/intercalation isotherms of CHT on the native Na^+-MMT particles (●) and MMT/POP hybrids (■) at 4 °C.

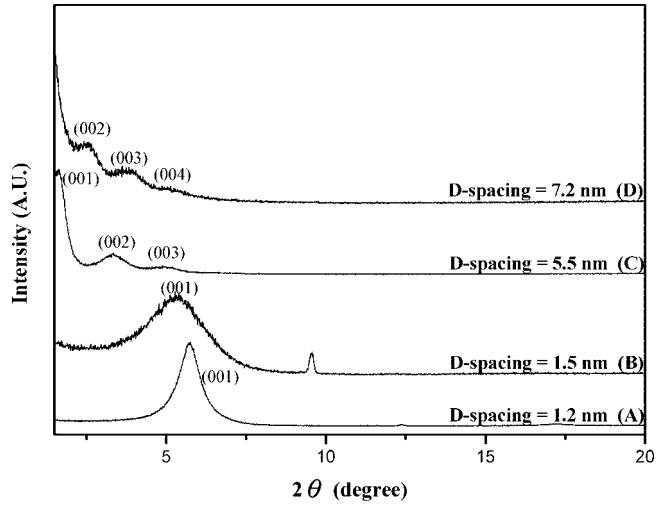

Figure 2. Powder XRD patterns of the native Na^+-MMT particles before (A) and after (B) CHT adsorption (65 μmol/g clay) and of the MMT/POP hybrids before (C) and after (D) the CHT intercalation/adsorption (MMT/CHT; 176 μmol/g clay).

RESULTS AND DISCUSSION

The intercalation/adsorption of CHT on MMT/POP particles significantly enhances the amount of CHT incorporated into the particles to 176 μmol/g clay (the saturation point) in comparison with that of only 65 μmol/g clay on native Na^+-MMT particles, as evidenced by two different adsorption isotherms in Figure 1. The adsorption behavior of CHT on Na^+-MMT particles is described well by the ideal Langmuir adsorption model as shown in the Supporting Information. In addition, after the CHT adsorption, the basal spacing of the clay particles was only slightly enlarged from 1.2 to ca. 1.5−2.2 nm by X-ray diffraction characterization (Figure 2). Apparently, the narrow interlayer space of Na^+-MMT particles (0.2 nm) fails to accommodate the globular CHT molecules with an original dimension of ca. $5 \times 6 \times 6$ nm^3, and the adsorption of protein species occurs to

a significant extent through the electrostatic interactions with the external particle surfaces (*10, 11, 17*). On the other hand, owing to the enlarged basal spacing of the clay layered particles by POP intercalation from 1.2 to ca. 5.5 nm (Figure 2), the complex isotherm of interacting CHT with the MMT/POP nanohybrids exhibits two different phases with respect to the simple Langmuir-type adsorption of CHT on Na^+-MMT. In the first phase, where the adsorption/intercalation amount is less than 86 μmol/g, the protein molecules are significantly adsorbed on the external surfaces of the multilayered particles. With only few CHT molecules being intercalated into each interlayer gallery, the basal spacing originally expanded by POP was slightly reduced (Supporting Information) due to the significant release of POP without sufficient incorporation of CHT. At an adsorption/intercalation extent of 80 μmol/g clay, it was observed that more than 40% of the POP molecules originally intercalated were released and the basal spacing was decreased from the initial 5.5 to 5.2 nm. Further expansion of the basal spacing to 7.2 nm was accomplished (Figure 2) by the enzyme entrapment amounting to 86 μmol/g (referred to as the critical point signifying the onset of the second phase) with the initial enzyme concentration in slurry at 440 μM. The basal spacing thereafter remained at ca. 7.2 nm, while the protein intercalation continued to proceed until equilibrium saturation was reached (Supporting Information). The expanded interlayer space of MMT/CHT at 6.2 nm is consistent with the molecular dimension of CHT, but significantly larger than those (with the basal spacing enlarged to a range of only 1.5−3.0 nm) by external surface adsorption and partial intercalation of various large protein molecules in previous reports (*18–21*). Herein, the extents of CHT (65 μmol/g clay at the saturation point) adsorbed on the surfaces of external plates of the Na^+-MMT particles and partially intercalated within their galleries were estimated based upon the saturation adsorption/intercalation of CHT at 176 μmol/g clay via MMT/POP. Assuming that each clay particle consists of 10 aluminosilicate plates and the CHT molecules are adsorbed/intercalated evenly on each of the external plate surfaces (×2) and within each of galleries (×9) of individual particles via MMT/POP, the enzyme adsorption on the external plate surfaces of particles amounts to ca. 32 μmol/g clay. With the same amount (32 μmol/g) of CHT adsorbed on the external plate surfaces, the extent of the protein intercalation within the Na^+-MMT galleries is only 33 μmol/g with respect to that of 144 μmol/g via MMT/POP. It has been reported that partial intercalation of large protein molecules takes place primarily in the outer regions of the interlayer spaces of native MMT particles, which, in agreement with our findings, results in only a small shift to higher basal spacing and a broadening of the d_{001} peak in the XRD measurements (*21*). Since the protein intercalation within Na^+-MMT occurs only in the outer regions of the galleries, herein it is referred to as a portion of the external particle surface adsorption for convenience. It is noteworthy that the MMT/POP particles originally in an extensively aggregated state at ambient temperature due to the inherent lower critical solution temperature (ca. 16−19 °C) of POP in water became well-dispersed at 4 °C, at which the clay structure became accessible to the protein intercalation and the biological functions of the protein were well-preserved. After the intercalation of the protein and release of POP, the new nanohybrids became easily dispersed in aqueous phase at ambient temperature. The SPM characterization of the MMT/CHT nanohybrids beyond the critical point shows that the hybrids were expanded to ca. 62−68 nm in height (Figure 3), as compared to only ca. 15−22 nm of Na^+-MMT particles with the maximum external surface adsorption of CHT (Supporting Information). With the basal spacing of 7.2 nm and the protein adsorption on the particle external surfaces taken into account,

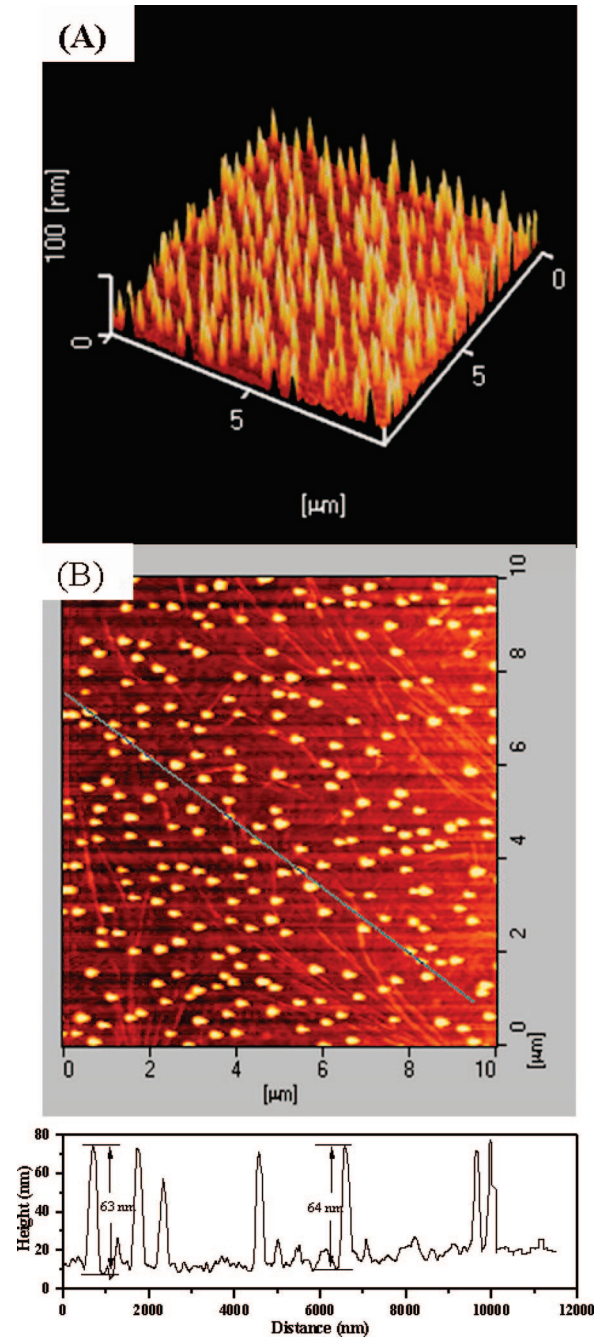

Figure 3. (A) Three dimensional AFM image and (B) the SPM topographical image of the MMT/CHT hybrids (176 μmol CHT/g clay) with lateral heights of ca. 62−68 nm.

the MMT/CHT nanohybrids are piling into ca. 8–10 platelets in a stack per particle. With further examination of the native Na^+-MMT and composite MMT/POP particles by SPM, the observations of the particle heights (ca. 11−13 and 40−45 nm, respectively, as shown in the Supporting Information) is in good agreement with the structure of 8−10 layers in a stack. Obviously, neither the intercalation of POP in Na^+-MMT nor exchange of the enzyme from the MMT/POP complexes leads to exfoliation of the clay multilayered structure.

Figure 4 illustrates the dependence of the enzyme activity in cleaving a small substrate, Bz-Tyr-NAp, on the extents of CHT intercalated and adsorbed on MMT particles (via MMT/POP and Na^+-MMT), respectively, at constant enzyme (2×10^{-7} M) and substrate (1.67×10^{-4} M) concentrations at 37 °C for 1 h. For comparison, free CHT has shown the capability of catalyzing the hydrolysis of the substrate to 78% under identical

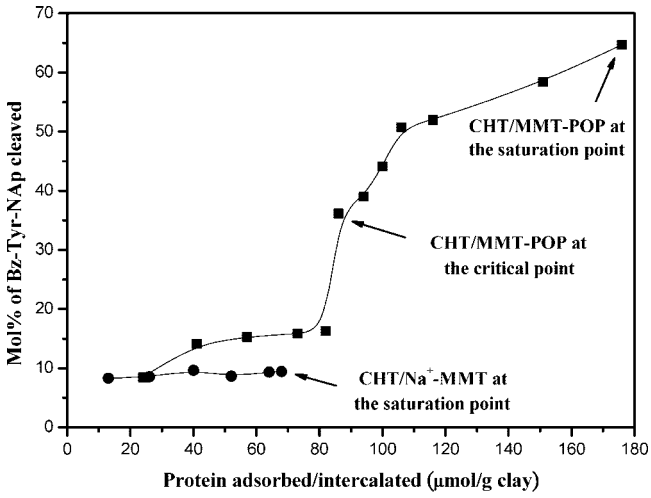

Figure 4. Dependence of the catalytic activity of CHT in hydrolyzing Bz-Tyr-NAp (mol %) on the extents of CHT adsorbed on Na^+-MMT particles (●) and intercalated within MMT/CHT hybrids (■). The reactions were carried out with a substrate concentration of 1.67×10^{-4} M at 37 °C for 1 h.

Table 1. Kinetic Parameters of the Cleavage of Two Small Substrates by Free CHT and MMT/CHT Hybrids[a]

Bz-Tyr-NAp	k_{cat} (s^{-1})	K_M (M) × 10^4	k_{cat}/K_M (s^{-1} M^{-1})
free CHT	0.437 ± 5.3%	1.60 ± 11.0%	2731 ± 10.0%
CHT/MMT-POP	0.422 ± 4.9%	3.15 ± 4.5%	1340 ± 2.3%
CHT/Na^+-MMT	0.288 ± 6.9%	3.70 ± 5.0%	778 ± 7.7%
Su-Phe-NAp	k_{cat} (s^{-1})	K_M (M) × 10^4	k_{cat}/K_M (s^{-1} M^{-1})
free CHT	0.182 ± 1.1%	7.00 ± 2.9%	257 ± 1.0%
CHT/MMT-POP	0.185 ± 3.2%	15.20 ± 5.8%	120 ± 4.3%
CHT/Na^+-MMT	0.084 ± 6.3%	17.20 ± 8.0%	49 ± 7.2%

[a] The extents of CHT intercalated in the MMT/CHT hybrids were 176 μmol/g clay and of adsorbed on external Na^+-MMT surfaces 65 μmol/g clay.

conditions. Independent of the extent of CHT adsorbed on the Na^+-MMT external particle surfaces, the enzyme shows reduced but constant activity. On the other hand, the MMT/CHT hybrids first show relatively low activity at the extents of the CHT intercalation below the critical point (86 μmol/g clay), where most CHT molecules reside on the external particle surfaces, and then abruptly enhanced activity beyond the critical point. Apparently, the spatially enlarged host galleries are essential for the enzyme to preserve its conformation and activity. The enzymatic activity continued to increase thereafter with increasing ratio of CHT embedded in the galleries to that adsorbed on the external particle surfaces until saturation of the CHT intercalation was achieved. Based upon the Michaelis–Menten kinetic theory, the kinetic parameters of the MMT/CHT hybrids in hydrolyzing two small substrates are listed in Table 1. The intercalated enzyme exhibits essentially identical catalytic activity (k_{cat}) to its free counterpart. However, the Michaelis constants (K_M) in interaction of both substrates increase significantly compared to the free enzyme. This can be ascribed to the reduced rate constant (k_1) in forming the enzyme/substrate complexes due to more retarded diffusion of the nonpolar substrates within the hybrids than that in bulk aqueous phase. In contrast, the enzyme suffers a dramatic reduction in activity (as signified by both the decreased k_{cat} and the increased K_M) when they are immobilized on the external particle surfaces of Na^+-MMT. The fully preserved activity of the intercalated CHT molecules within the clay galleries can be accounted for by the salt-bridge effect resulting from the electrostatic interactions of the enzyme molecules with negatively charged platelets of both top and bottom sides on stabilizing the native conformation of the protein in a manner similar to that of the engineered proteins (*4, 22*). Confinement of the enzyme molecules within the rigid clay galleries may additionally protect the protein from unfolding by steric hindrance (*23*). The protein conformation can also be partially stabilized by reducing the activity of water molecules in the galleries and therefore reducing the extents of hydration of the nonpolar groups of the intercalated proteins and of dehydration of their polar groups, which is suggested to be essential for protein unfolding (*4, 24*). On the other hand, owing to the absence of the electrostatic interactions with both the top and bottom platelet surfaces, the enzyme molecules, when being adsorbed on the Na^+-MMT external plate surfaces, can be more easily denatured. In addition, it is expected that the conformation of the CHT molecules intercalated in the outer regions of the Na^+-MMT galleries be largely perturbed due to the compressive effects of the inorganic platelets with the narrow basal spacing of 1.5−2.2 nm. Similar results on the reduction of catalytic activity of the enzymes upon immobilization on MMT surfaces have been observed and ascribed to the perturbation of protein conformation and modification of their active centers, mostly using the FTIR measurements (*10, 19–21, 25, 26*).

Taking advantage of CHT as a protease, the clay/enzyme nanohybrids were tested for their residual activity toward Bz-Tyr-NAp after preincubating the clay/enzyme suspensions alone for 1 h at varying temperatures. Figure 5A shows the relative activity of CHT in varying forms (the free, externally adsorbed, and intercalated, respectively) after preincubation at different temperatures to that preincubated at 5 °C as a function of the extent of intercalation (via MMT/POP) or external particle surface adsorption (via Na^+-MMT) at a constant enzyme concentration (2.0×10^{-7} M) in solutions. Figure 5B emphasizes the effects of the enzyme concentrations (1.0×10^{-6} and 2.0×10^{-7} M) in solutions, while the extent of CHT intercalated (100 μmol/g) or adsorbed (41 μmol/g) was kept unchanged. With increasing enzyme concentration and preincubation temperature (up to 55 °C, the temperature for the optimal activity of CHT, both the free and intercalated), the degree of reduction in the relative activity of the free CHT increases primarily as a result of the proteolytic action on CHT molecules themselves (self-digestion). In contrast, for the CHT adsorbed on the external surfaces of Na^+-MMT particles, the activity profile upon preincubation was independent of both the enzyme concentration and the adsorption extent, strongly indicative of the lack of significant self-interactions and -digestion of the enzyme molecules. The observed temperature effect on the reduction in the activity of CHT adsorbed on the external particle surfaces is attributed to thermally facilitated protein denaturation on the external surfaces of inorganic particles. On the other hand, the residual activity of the intercalated CHT is influenced markedly by both the preincubation temperature and the intercalation extent at a constant enzyme concentration, but is insensitive to change in the enzyme concentration in solutions for the MMT/CHT nanohybrids of a certain extent of enzyme intercalation. Similar to free CHT, the change of the relative activity is caused significantly by self-digestion, but occurs within the nanohybrids exclusively. Strong dependence of self-cleavage on the intrinsic concentration of enzyme within the nanohybrids was hence observed. However, one of the prerequisites for the protease molecules to self-digest so extensively in their medium relies more likely on their ability to migrate freely to interact with each other. Owing to negative charges evenly distributed throughout the plate interior surfaces, enzyme molecules residing in the galleries retain not only the native structure but also the mobility in sliding in a two-dimensional manner within the confinement without deterioration of the electrostatic attractions. The difference in the concentrations between the intercalated CHT within the nanohybrids and the

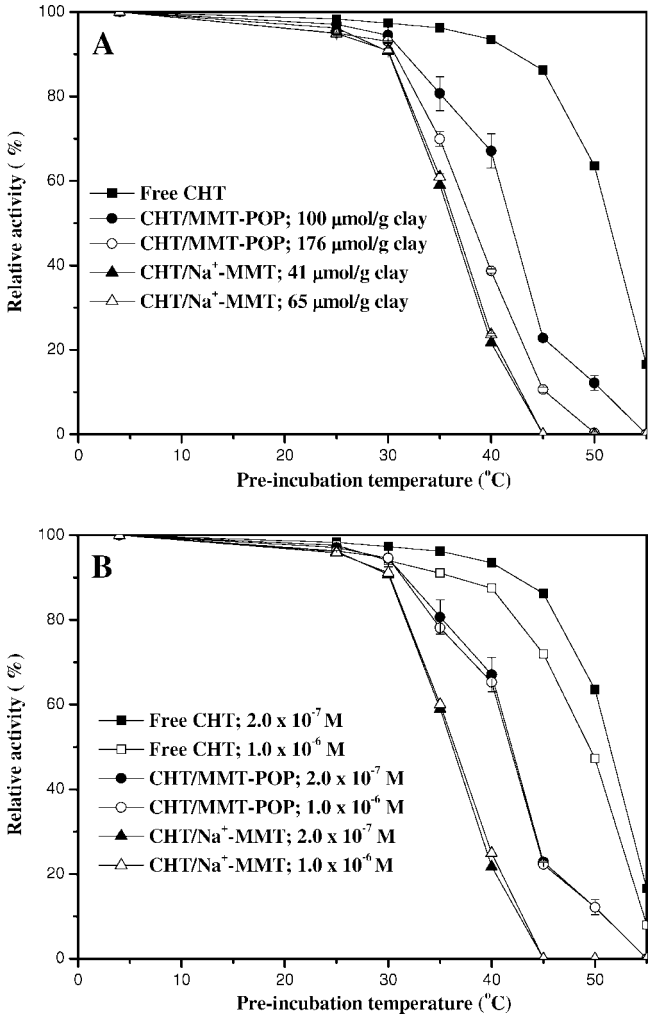

Figure 5. Effects of the preincubation of the aqueous solution of CHT in the free, intercalated (via MMT/POP hybrids), and adsorbed (on Na^+-MMT particles) forms at varying temperatures on relative residual activity in hydrolyzing Bz-Tyr-NAp to that of the preincubation at 5 °C as functions of (A) the extents of CHT intercalated and adsorbed at a constant enzyme concentration (2.0×10^{-7} M) and (B) of the enzyme concentration with the constant extents of intercalation at 100 μmol/g clay (via MMT/POP) and of external adsorption at 41 μmol/g clay (Na^+-MMT), respectively.

free counterpart in aqueous solution also leads to varying degrees of self-digestion and therefore the residual activity. It should be noted that the self-digestion occurs usually by proteases only and is not observed from nonproteolytic enzymes, including those employed for protein therapeutics and biomedical applications.

The interaction of CHT within the hybrids with biomacromolecules was characterized in terms of the extent of proteolytic cleavage of protein–substrates (BSA and catalase, respectively) by incubating with the MMT/CHT particles in aqueous solutions. The degradation was evaluated by monitoring the change in the molecular peaks of protein–substrates from the GPC measurements with time. Figure 6 shows that catalase was only degraded slightly (<18% in the molecular cleavage) by the MMT/CHT nanohybrids within an incubation time interval of 72 h while extensive proteolysis (>92%) occurred by the free CHT. Similarly, BSA, being employed as the other macromolecular substrate, was severely restricted to interacting with the CHT molecules embedded within the galleries of the MMT particles in comparison with its rapid digestion by the free enzyme (Supporting Information). The restriction of interacting the intercalated CHT molecules with biomacromolecular substrates is caused primarily by both the steric hindrance of the inorganic host plates in the layered structure and the limited free space remaining within the host galleries in addition to the CHT occupation. The observed proteolytic action of the MMT/CHT hybrids on both catalase and BSA is most probably due to the accessibility of the CHT molecules that reside on the external particle surfaces (including the outer regions of the clay galleries) to interaction with the substrates. Morphologic examination of the MMT/CHT nanohybrids after incubating with catalase by SPM demonstrates that the lateral heights of

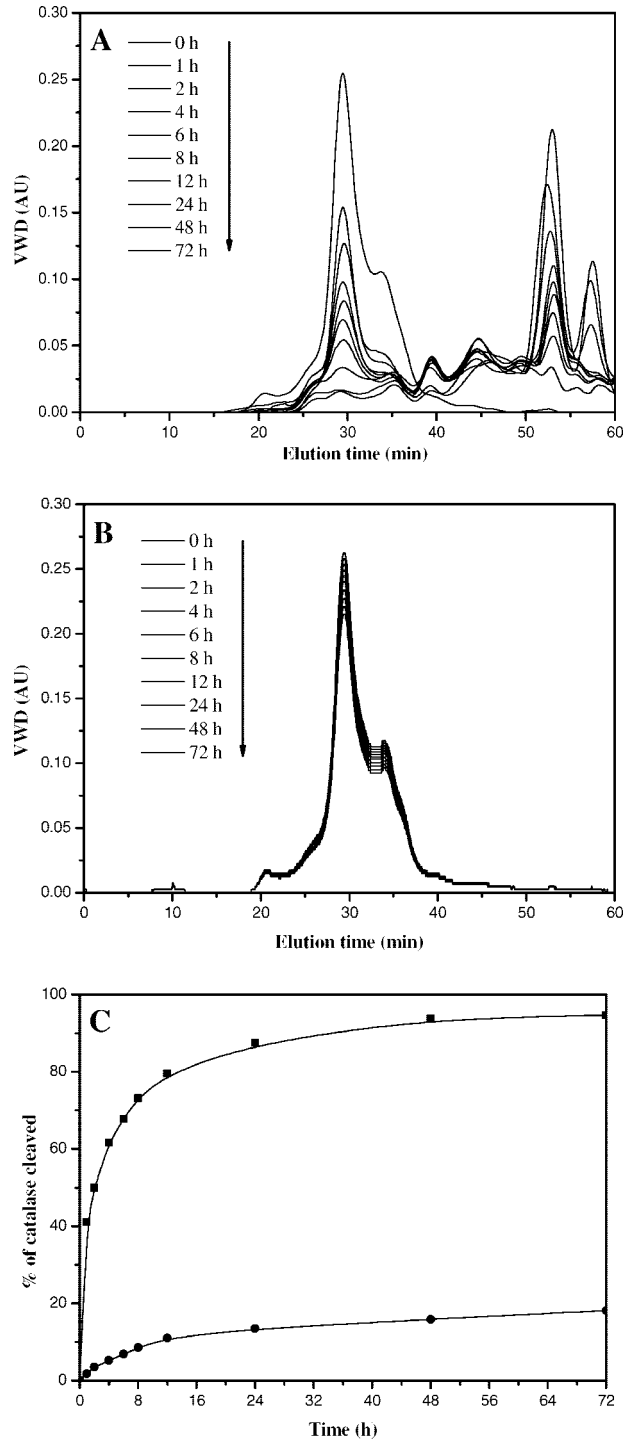

Figure 6. GPC spectra of catalase as a function of the incubation time with (A) the free CHT and (B) MMT/CHT hybrids (176 μmol/g clay), respectively. (C) Cleavage extents of catalase in terms of the decreases (%) of the molecular peak height of catalase by proteolytic action of the free CHT (■) and MMT/CHT hybrids (●) with time.

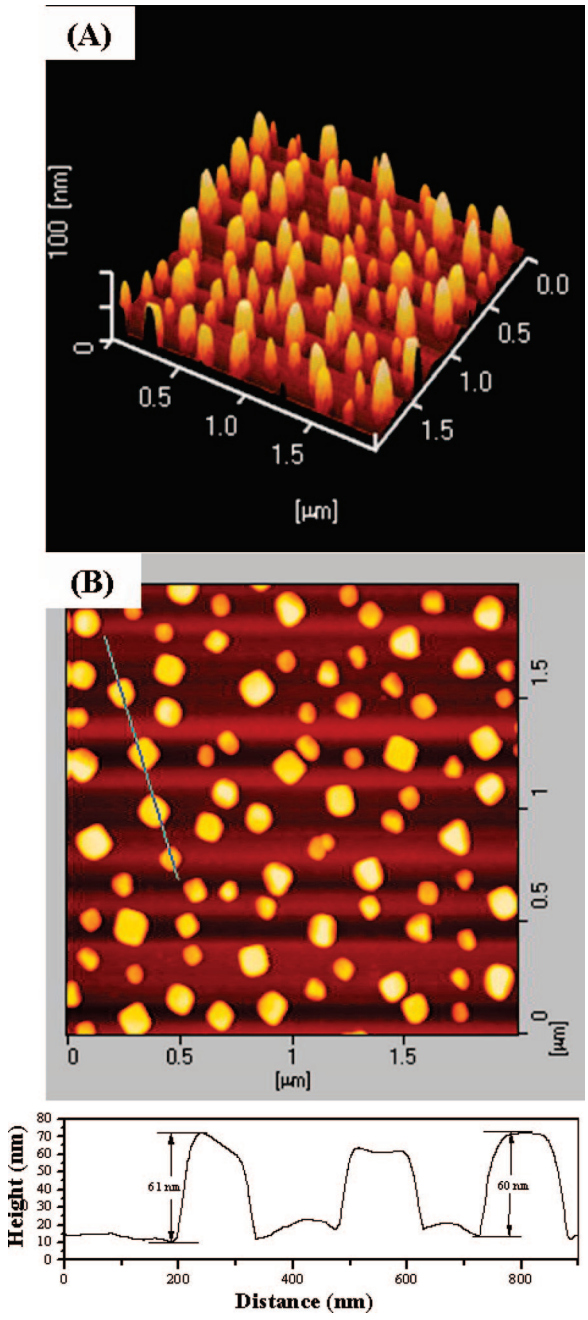

Figure 7. (A) Three-dimensional AFM image and (B) the SPM topographical image of the MMT/CHT hybrids (176 μmol/g clay) with lateral heights of ca. 60∼70 nm after incubation with catalase for 72 h.

the nanohybrids in the range 60−70 nm were essentially the same as those prior to the incubation reactions (Figure 7). Similar observation was obtained from the incubation of the hybrids with BSA (Supporting Information). The results further suggest that neither exfoliation of the clay multilayered structure nor exchange with the originally intercalated CHT occur by catalase and BSA in approaching the MMT/CHT hybrids, although the latter has been found capable of being intercalated in the galleries of MMT/POP via cationic exchange with POP (*27*). It has been confirmed that the expansion of the basal spacing from 1.2 to 5.5 nm with the POP intercalation to a critical extent is supported mainly by significant hydrophobic segregation of the polymer strains in aqueous medium within the gallery (*15*). The different fates of BSA while in contact with MMT/POP and MMT/CHT hybrids suggest that the stability of the inorganic layered structure becomes enhanced by accommodating protein molecules within the galleries due to the more extensive electrostatic attractions with negatively charged platelets on both top and bottom sides and the more compact hydrophobic association of the protein globular structure in nature. Therefore, it is not surprising that the CHT molecules originally intercalated within the clay multilayered structure underwent conformational change by placing the lyophilized hybrids in organic solvents, such as DMSO, leading to inactivation of the enzyme molecules and exfoliation of the clay layered structure (data not shown).

The MMT/CHT nanohybrids reported herein have shown similarity in several aspects to PEG−enzyme adducts. The enzyme molecules residing within the galleries of the MMT particles most likely retain their structure in the native conformation. However, the enzyme functions are tailored such that the enzymatic activity toward small substrates can be fully preserved and interactions with the approaching biomacromolecules effectively inhibited. On the other hand, the hybrids in nanoscale render themselves particularly useful when fixation or immobilization is strongly preferred. This nanoscaled manipulation of enzyme functions through a clay accommodation and immobilization can be a valuable approach whereby hybrids of therapeutically active enzymes with preference for activity only in small substrates can possibly be developed as new therapeutics or bioreactors in tissue engineering, taking advantage of their easy fixation and reduced interactions with biomacromolecules, including those responsible for proteolytic action and immune response.

CONCLUSIONS

The MMT/enzyme nanohybrids obtained by a facile exchange process of the enzyme molecules with POP in space-enlarged galleries of MMT/POP have shown the capability of retaining the layered structure of the inorganic host and enzymatic activity of the guest molecules in hydrolyzing small substrates while rejecting interactions with large biomacromolecules. The capacity in accommodating protein within clay galleries is much larger than that by only adsorption on the external surfaces of Na^+-MMT particles. In addition, the stability of the layered structure of MMT/CHT nanohybrids can be further enhanced as compared to MMT/POP, leading to the observation that neither exchange nor exfoliation occurred when the hybrids were in contact with other proteins. This study indicates that, through the accommodation capability of clay, the simple nanoscaled manipulation of protein functions can be highly useful in developing new clay/enzyme nanohybrids for protein therapeutics and tissue engineering.

ACKNOWLEDGMENT

This work is supported in part by the National Science Council and the Ministry of Education of Taiwan under the ATU plan.

Supporting Information Available: The Langmuir-type adsorption isotherm of CHT on Na^+-MMT, the XRD diffraction patterns of MMT/CHT nanohybrids with varying extents of intercalation, the three-dimensional AFM images and the SPM topographical images of Na^+-MMT, CHT-adsorbed Na^+-MMT, MMT/POP, and MMT/CHT hybrids after incubating with BSA and the enzymatic degradation of BSA by free CHT and MMT/CHT nanohybrids. This material is available free of charge via the Internet at http://pubs.acs.org.

LITERATURE CITED

(1) Choy, J.-H., Kwak, S.-Y., Jeong, Y.-J., and Park, J.-S. (2000) Inorganic layered double hydroxides as nonviral vectors. *Angew. Chem. Int. Ed. 39*, 4041–4045.

(2) Desigaux, L., Belkacem, M. B., Richard, P., Cellier, J., Léone, P., Cario, L, Leroux, F, Taviot-Gueho, C., and Pitard, B. (2006) Self-assembly and characterization of layered double hydroxide/DNA hybrids. *Nano Lett. 6*, 199–204.

(3) Kumar, C. V., and Chaudhari, A. (2000) Protein immobilized at the galleries of layered α-zirconium phosphate: Structure and activity studies. *J. Am. Chem. Soc. 122*, 830–837.

(4) Kumar, C. V., and Chaudhari, A. (2002) High temperature peroxidase activities of HRP and hemoglobin in the galleries of layered Zr(IV) phosphate. *Chem. Commun.* 2382–2383.

(5) Kumar, C. V., and Chaudhari, A. (2003) Unusual thermal stabilities of some proteins and enzymes bound in the galleries of layered α-Zr(IV)phosphate/phosphonates. *Microporous Mesoporous Mater. 57*, 181–190.

(6) Bellezza, F., Cipiciani, A., Costantino, U., Negozio, and M, E. (2002) Zirconium phosphate and modified zirconium phosphates as supports of Lipase. Preparation of the composites and activity of the supported enzyme. *Langmuir 18*, 8737–8742.

(7) Bellezza, F., Cipiciani, A., Costantino, U., and Nicolis, S. (2004) Catalytic activity of myoglobin immobilized on zirconium phosphonates. *Langmuir 20*, 5019–5025.

(8) Bellezza, F., Cipiciani, A., Costantino, U., and Marmottini, F. (2006) Adsorption of myoglobin onto porous zirconium phosphate and zirconium benzenephosphonate obtained with template synthesis. *Langmuir 22*, 5064–5069.

(9) Kumar, C. V., and Chaudhari, A. (2001) Efficient renaturation of immobilized Met-hemoglobin at the galleries of α-zirconium phosphate. *Chem. Mater. 13*, 238–240.

(10) Baron, M. H., Revault, M., Servagent-Noinville, S., Abadie, J., and Quiquampoix, H. (1999) Chymotrypsin adsorption on montmorillonite: Enzymatic activity and kinetic FTIR structure analysis. *J. Colloid Interface Sci. 214*, 319–332.

(11) Ding, X., and Henrichs, S. M. (2002) Adsorption and desorption of proteins and polyamino acids by clay minerals and marine sediments. *Mar. Chem. 77*, 225–237.

(12) Usuki, A., Hasegawa, N., Kadoura, H., and Okamoto, T. (2001) Three-dimensional observation of structure and morphology in Nylon-6/clay nanocomposite. *Nano Lett. 5*, 271–272.

(13) Lin, J.-J., Cheng, I.-J., Wang, R., and Lee, R.-J. (2001) Tailoring basal spacings of montmorillonite by poly(oxyalkylene)diamine intercalation. *Macromolecules 34*, 8832–8834.

(14) Chou, C.-C., Shieu, F.-S., and Lin, J.-J. (2003) Preparation, organophilicity, and self-assembly of poly(oxypropylene)amine-clay hybrids. *Macromolecules 36*, 2187–2189.

(15) Lin, J.-J., Chen, I.-J., and Chou, C.-C. (2003) Critical conformational change of poly(oxypropylene)diamines in layered aluminosilicate confinement. *Macromol. Rapid Commun. 24*, 492–495.

(16) Chiu, H.-C., Zalipsky, S., Kopečková, P., and Kopeček, J. (1993) Enzymatic activity of chymotrypsin and its poly(ethylene glycol) conjugates toward low and high molecular weight substrates. *Bioconjugate Chem. 4*, 290–295.

(17) Mattews, B. W., Sigler, P. B., Henderson, R., and Blow, D. M. (1967) Three-dimensional structure of tosyl-α-chymotrypsin. *Nature (London) 214*, 652–656.

(18) Cristofaro, A. D., and Violante, A. (2001) Effect of hydroxy-aluminum species on the sorption and interlayering of albumin onto montmorillonite. *Appl. Clay Sci. 19*, 59–67.

(19) Calamai, L., Lossi, I., Stotzky, G., Fusi, P., and Ristori, G. G. (2000) Interaction of catalase with montmorillonite homoionic to cations with different hydrophobicity: Effect on enzymatic activity and microbial utilization. *Soil Biol. Biochem. 32*, 815–823.

(20) Naidja, A., and Huang, P. M. (1996) Deamination of aspartic acid by aspartase-Ca-montmorillonite complex. *J. Mol. Catal., A: Chem. 106*, 255–265.

(21) Fusi, P., Ristori, G. G., Calamai, L., and Stotzky, G. (1989) Adsorption and binding of protein on "clean" (homoionic) and "dirty" (coated with Fe oxyhydroxides) montmorillonite, Illite and kaolinite. *Soil Biol. Biochem. 21*, 911–920.

(22) Spek, E. J., Bui, A. H., Lu, M., and Kallenbach, N. R. (1998) Surface salt bridges stabilize the GCN4 leucine zipper. *Protein Sci. 7*, 2431–2437.

(23) Zhou, H.-X., and Dill, K. A. (2001) Stabilization of proteins in confined spaces. *Biochemistry 40*, 11289–11293.

(24) Khechinashvili, N. (1990) Thermodynamic properties of globular proteins and the principle of stabilization of their native structure. *Biochim. Biophys. Acta, Protein Struct. Molec. Enzym. 1040*, 346–354.

(25) Naidja, A., Huang, P. M., and Bollag, J.-M. (1997) Activity of tyrosinase immobilized on hydroxylaluminum-montmorillonite complex. *J. Mol. Catal., A: Chem. 115*, 305–316.

(26) Asthagiri, D., and Lenhoff, A. M. (1997) Influence of structure details in modeling electrostatically driven protein adsorption. *Langmuir 13*, 6761–6768.

(27) Lin, J.-J., Wei, J.-C., Juang, T.-Y., and Tsai, W.-C. (2007) Preparation of protein-silicate hybrids from polyamine intercalation of layered montmorillonite. *Langmuir 23*, 1995–1999.

BC700224Q